13

A novel method of plasmon coupled optical waveguide for aerosol sensor

© Sushil Kumar[1], Gaurav Sharma[2], Gulab Chand Yadav[2], Vivek Singh[2], Abhay Kumar Singh[2]

[1] Department of Physics, Sri Shankar College Sasaram (Constituent Body of Veer Kunwar Singh University Ara), Rohtas, Bihar 821115, India
[2] Department of Physics, Institute of Science, Banaras Hindu University, Varanasi, Uttar Pradesh 221005 India

Received January 09, 2021
Revised July 07, 2021
Accepted July 28, 2021

The tropospheric aerosol characterization is important for understanding environmental process as well as human health safety. In this study, the surface plasmon resonance sensor is proposed for the detection of ammonium sulfate which is an important component of aerosols. The reflectivity of proposed sensor waveguides is calculated as a function of the incident angle using the transfer matrix method. The performance of proposed sensors having sol-gel film of tetraethylorthosilane and thymolblue are studied and compared. Firstly, the dispersion characteristics are obtained for different modes, and it is observed that the modes are tightly bound in thymol blue waveguide in comparison to tetraethylorthosilane waveguide. Further, the magnetic field distributions are also studied and compared for proposed waveguide sensor configurations. It is found that the sol-gel film of thymol blue waveguide provides high sensitivity while tetraethylorthosilane waveguide shows high figure of merit.

Keywords: aerosol, surface plasmon resonance sensor, reflectivity, sensitivity, detection accuracy.

DOI: 10.21883/EOS.2022.14.54000.1014-21

1. Introduction

Tropospheric aerosols have large influence on air quality of environment, reductions in visibility of atmosphere and the earth.s climate. The chemical compositions of aerosols play an important role in cloud processes as well as a health issue in urban and rural areas [1–2]. Therefore, it is necessary to detect aerosol composition with great accuracy. The vast chemical composition of aerosol consists of elementary carbon, organic carbon as well as inorganic species such as soot, sulfates, nitrates and ammonium. Among these compositions, the ammonium sulfates (AS) is the one of most common constituents of aerosols, which has its fraction of 22% [3–5]. AS particles are the major constituents in the atmosphere and their detection is important to check the quality of air. It is observed that a large portion of the inorganic sulfates is in the form of AS aerosols that affect the vegetation [6] and a pathway for atmospheric ice nucleation [7–8]. The various methods like four-stage photo-oxidation [9] chemical ionization mass spectrometry [10] and gas chromatography/ion trap mass spectrometry [11] has been used to characterise the chemical composition of aerosols. Airborne aerosols sampling technology and other analytical techniques have their limitations in sampling. Also, most of the measuring methods for aerosol chemical compositions depend on mass spectroscopic techniques which are costly, allow laboratory analysis and time-consuming. Kalberer et al. use different polymerization reactions to identify the polymers that affects aerosol properties such as optical parameters, hygroscopic growth, and cloud condensation [12]. Besides the mass spectroscopy, the optical techniques such as LIDAR (light detection and ranging) showed the powerful tool for observation of atmospheric aerosol from surface to the upper atmosphere. In this regard the optical characterizations have been used to find the chemical species in tropospheric aerosol using cavity ring down spectroscopy i.e ellipsometry and interferometeric [13]. Further, the fiber optic sensor based on evanescent wave absorption technique for the detection of the chemical composition of the aerosol is also presented by a group of researchers [14].

However, large number of chemical sensors has been studied for environmental monitoring, but there is a need for versatile, low cost, accurate, lightweight and small size sensor for continuous monitoring. The surface plasmon resonance (SPR) sensor is one of the best techniques for long-term monitoring that can be operated on real-time measurement of aerosols [15,16]. The key advantage of the SPR sensor is user friendly, offers many other advantages such as easy use, reliable and fast response. From the last decade, many works have been carried out to improve the performance of the SPR sensor [17–18]. Kretschmann.s configuration is commonly used in SPR sensing because in this configuration, a thin layer of silver or gold metal is coated on the glass substrate after that a film is depositedon the metal surface that is sensitive for targeted chemical. Therefore, in this communication, Kretschmann.s configuration of SPR technique is used to investigate AS. Here two sol-gel film either Tetraethylorthosilane (Ts) or Thymol Blue (Tb) is deposited on gold metal surface to detect AS, and their performance are analysed and compared. The paper is arranged in the following sections. Section 2 provides the theoretical description of principle of surface plasmon resonance sensor with the performance analysis parameters. In section 3, the numerical simulations

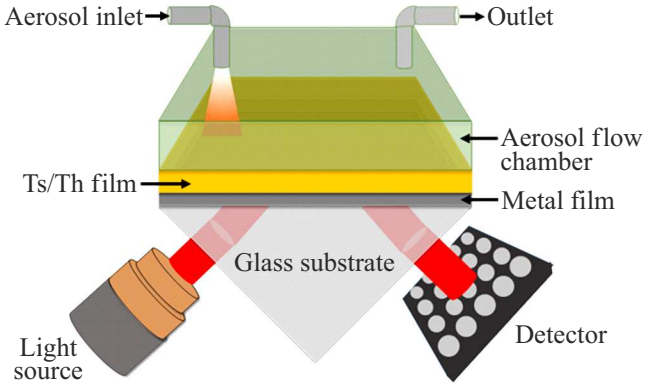

Figure 1. Schematic diagram of proposed plasmonicsensing system.

results are discussed and compared. Finally, the conclusion is drawn in section 4.

2. Theoretical Description

A schematic diagram of the proposed sensor configuration is shown in Fig. 1. In this study,two waveguide sensor configurations are proposed. First waveguide sensor consists of the prism as substrate, Ag metal and the sol-gel film of tetraethylorthosilane. The second proposed waveguide sensor structure consists of prism as substrate, Ag metal and the sol-gel film of thymol blue.We considered p-polarized light beam incident on the prism consists of metal and the sol-gel film of Ts or Tb. According to the Maxwell equation, the wave vector of incident light and surface plasmon wave is given as

$$k_s = \frac{\omega}{c}\sqrt{\varepsilon_p} \quad \text{(incident light)}, \tag{1}$$

$$k_{sp} = \frac{\omega}{c}\sqrt{\frac{\varepsilon_m \varepsilon_s}{\varepsilon_m + \varepsilon_s}} \quad \text{(surface plasmon wave)}, \tag{2}$$

where ε_p, ε_m and ε_s represents the respected dielectric constant of prism, metal, and sensing resign, ω is the frequency of the incident light and c the free space velocity ofthe light. Since the wave vector of the incident light inair islargerthan the wave vector of the surface plasmon wave. Therefore, the incident light is passed througha high refractive index substrate at different incidence angles larger than the critical angle. The wave vector of incident light after the passing through a prism at different angle is given by

$$k_{ev} = \frac{\omega}{c}\sqrt{\varepsilon_p}\sin\theta. \tag{3}$$

The SPR occurs when the wave vector of the incident light along the interface becomes equal to the wave vector of the surface plasmon wave ($k_{ev} = k_{sp}$). Hence if the frequency of incident light is fixed, then at a particular angle θ_{res}, the resonance condition is expressed as

$$\frac{\omega}{c}\sqrt{\varepsilon_p}\sin\theta_{\text{res}} = \frac{\omega}{c}\sqrt{\frac{\varepsilon_m \varepsilon_s}{\varepsilon_m + \varepsilon_s}}. \tag{4}$$

Equation (4) shows that the resonance condition depends on many parameters such as the angle of incident light, frequency of the used light, refractive index of glass substrate, metal and the sensing media. Surface plasmon wave represents transverse magnetically polarized waves that travel along with the interface, and the field associated with these waves decays exponentially.

The Fresnel amplitude reflection coefficient of the waveguide is calculated by using the transfer matrix method of K-layer systems [19]. In a multilayer structure assumed that each layer having arbitrarythickness d_k, refractive index n_k and dielectric constant ε_k. In this method, the field at first boundary isrelated tothe last boundary as given below [20,21]

$$\begin{bmatrix} U_1 \\ V_1 \end{bmatrix} = M \begin{bmatrix} U_{N-1} \\ V_{N-1} \end{bmatrix}, \tag{5}$$

where U_1, V_1 and U_{N-1}, V_{N-1} are the respective tangential electric field component at the first boundary and last layer boundary. M is called as characteristic matrix of combined structure and expressed as

$$M = \prod_{k=2}^{N-1} M_k = \begin{bmatrix} M_{11} & M_{12} \\ M_{21} & M_{22} \end{bmatrix},$$

$$M_k = \begin{bmatrix} \cos\delta_k & -i\sin\delta_k/\eta_k \\ -i\eta_k\sin\delta_k & \cos\delta_k \end{bmatrix}, \tag{6}$$

where δ_k, η_k are the phase factor and optically admittance, respectively. These factors are given as

$$\eta_k = \frac{(\varepsilon_k - n_1^2\sin^2\theta_1)^{1/2}}{\varepsilon_k}, \tag{7a}$$

$$\delta_k = \frac{2\pi d_k}{\lambda}(\varepsilon_k - n_1^2\sin^2\theta_1)^{1/2}, \tag{7textb}$$

where θ_1 and λ are the incident angle and the wavelength of the light.

Finally, the reflectivity of a given multilayer structure is given by

$$R_p = |r_p|^2, \tag{8}$$

where r_p is the amplitude of reflection of p-polarized light and expressed as

$$r_p = \frac{(M_{11} + M_{12}\eta_k)\eta_1 - (M_{21} + M_{22}\eta_k)}{((M_{11} + M_{12}\eta_k)\eta_1 + (M_{21} + M_{22}\eta_k)}. \tag{9}$$

The performance of the surface plasmon resonance sensor is evaluated in the term of sensitivity (S), detection accuracy (DA) and figure of merit (FOM). The sensitivity (S) is defined as the ratio of the change in resonance angle ($\delta\theta_{\text{res}}$), to the small change in refractive index sensing media (δn_s)

$$S = \frac{\delta\theta_{\text{res}}}{\delta n_s} \tag{10}$$

Detection Accuracy (DA) determines the accuracy of resonance angle measurement and defined as the reciprocal

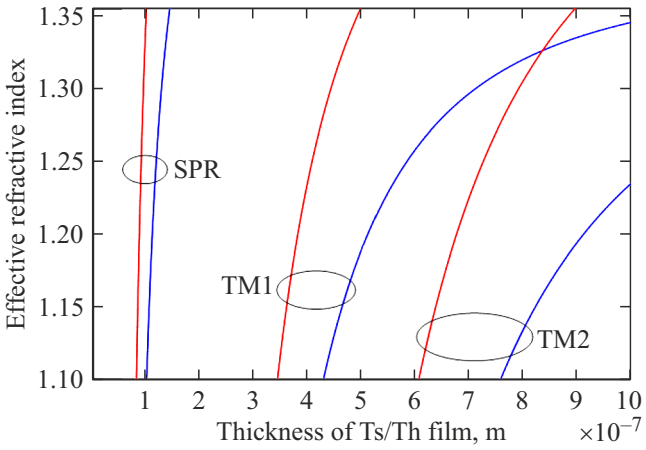

Figure 2. Dispersion characteristic of SMTs (blue colour) and SMTb (red colour) waveguide sensor.

of the full width at half maximum (FWHM) of the reflection dip:

$$DA = \frac{1}{\delta\theta_{0.5}}, \tag{11}$$

where $\delta\theta_{0.5}$ is the difference in the angle at 50%, reflectivity.

Here, the combinations of the sensitivity and detection accuracy are referred as the figure of merit (FOM). It is defined as the ratio of the sensitivity to the FWHM of the reflectance curve:

$$FOM = \frac{S}{\delta\theta_{0.5}}. \tag{12}$$

3. Numerical Simulation, Results and Discussion

The proposed waveguides consist of a glass substrate (S), metal layer (M) and a sol-gel film of Tetraethylorthosilane (Ts) or Thymol Blue (Tb) as shown in Fig. 1. Both of these configurations are used to detect AS and is denoted as SMTs and SMTb waveguide, respectively. All the numerical calculation is based on angular interrogation method with fixed incident wavelength 550 nm. The semi-infinite NSF-11 glass substrate with 50 nm gold thin film has the refractive index (RI) 1.77 and $0.105 + 3.107i$, respectively [22,23]. Above the gold layer, a thin film of Tb or Ts is deposited, which has the refractive index 1.32 and 1.52, respectively. Literatures suggest that the refractive index of AS varies from 1.43 to 1.55 depending upon the, size distribution of AS and density of the aerosol [3–5,24–27]. Figure 2 shows the dispersion characteristics of SMTs and SMTb waveguide by considering the 1.55 RIofAS. The dispersion characteristics of SMTs and SMTb waveguide is denoted as blue line and red line respectively. It is clear from Fig. 2 that the fields are loosely bounded in SMTs in comparison of SMTb waveguide, and the effective index in both waveguides varies according to the sol-gel film thickness. The cut-off thicknesses are tabulated in table 1

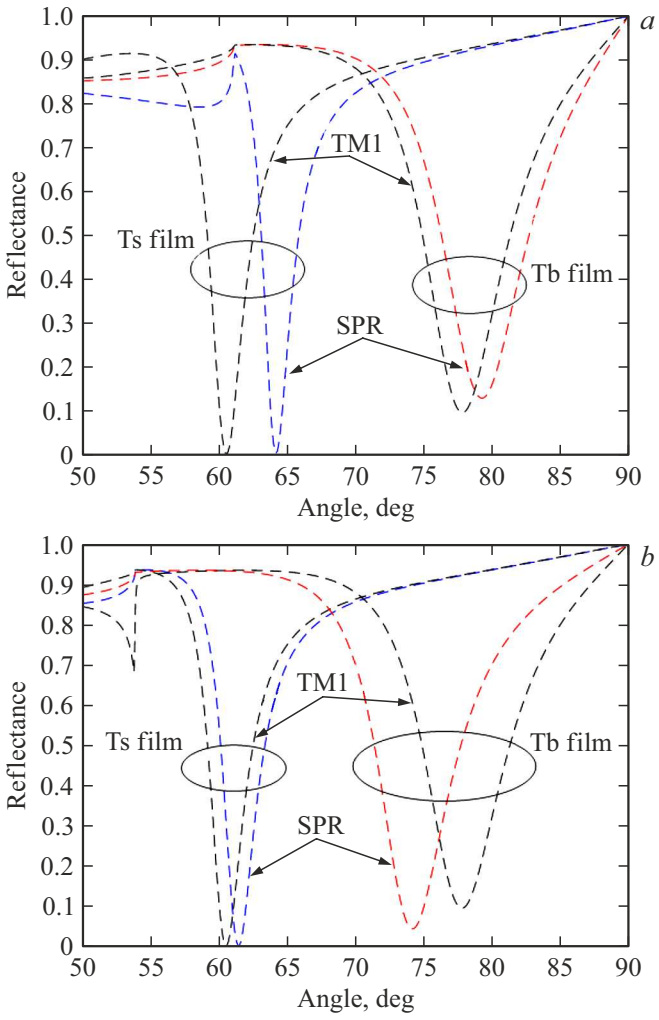

Figure 3. Calculated normalised reflectance with incidence angle for AS refractive index (a) 1.55 and (b) 1.43.

Table 1. The cutoff film thickness of proposed waveguides for three lower order modes

	Film thickness for Ts waveguide, nm	Film thickness for Tb waveguide in, nm
TM_0(SPR)	100	80
TM_1	430	340
TM_2	760	610

for TM0 (SPR), TM1 and TM2 mode. The difference in cut off thickness of SPR mode is 20 nm, and, for other modes this difference is very high.

The reflectance of SMTs waveguide sensor is calculated at fixed Ts film thickness 100 nm (TM_0) and 430 nm (TM_1). Similarly, the reflectance of SMTb waveguide sensor is calculated at fixed Tb film thickness 80 nm (TM_0) and 340 nm (TM_1). Fig. 3, a and Fig. 3, b shows the respective reflectance at 1.55 and 1.43 refractive index variation of AS for above two proposed waveguides. In Fig. 3, a, it is

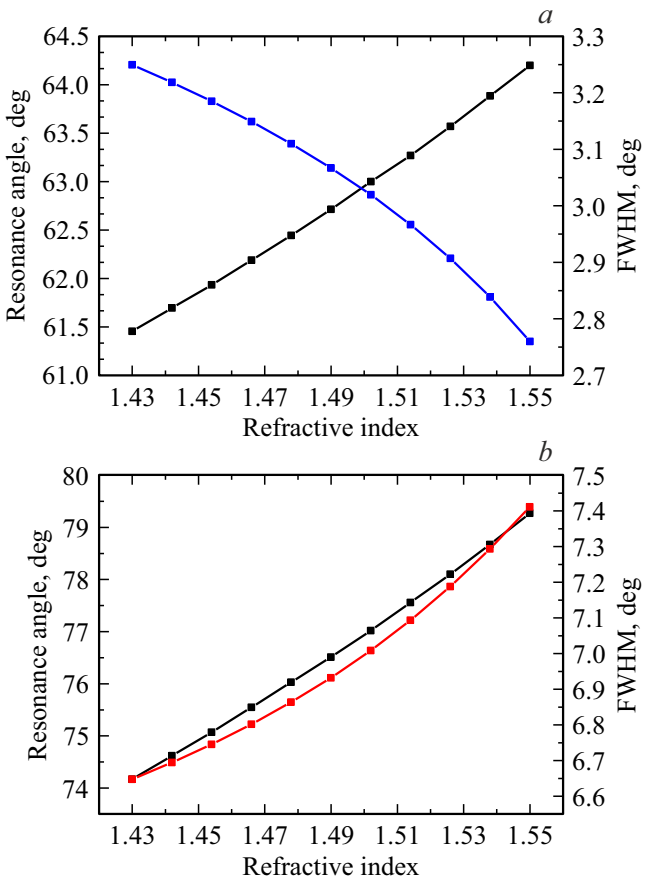

Figure 4. Calculation for variation of resonance angle and FWHM with refractive index of AS (a) SMTs Waveguide Sensor, (b) SMTb Waveguide Sensor.

observed that as increases the thickness of sol-gel film the resonance angle (dip) shifts towards lower angle for both SMTs and SMTb waveguides. In Fig. 3, *b*, it is clear that with increase the thickness of sol-gel film, the resonance angle shifts toward lower angle for SMTs waveguide but this resonance angle shifts towards higher angle for SMTb waveguide. It is because that a reverse symmetry is produced for lower refractive index of AS by the film refractive index of Tb. The similar calculations of normalised reflectance have been made for the small change of AS layer refractive index and calculate the performance parameter of the sensor in term of sensitivity (S) and detection accuracy (DA). The performance parameter for SPR (TM_0), TM_1 and TM_2 mode are calculated at AS refractive index 1.55 and 1.43 and tabulated in table 2. This table indicates that SPR mode provides better performance parameters in comparison of TM_1 and TM_2 modes. The maximum sensitivity is achieved 50°/RIU in SMTb waveguide sensor and maximum detection accuracy is 0.36/deg in SMTs waveguide sensor at 1.55 AS refractive index. Figure 4, *a* shows the resonance angle and FWHM variation for SMTs waveguide sensor withRI of AS. It is clear that resonance angleincreases and FWHM decreaseswith increased AS refractive index. The calculated range of resonance angle is obtained 61.45° to 64.54° and the range of FWHM is obtained 3.24° to 2.66°. Similar calculations have been made for SMTb waveguide configuration as shown in Fig. 4, *b* and it is found that resonance wavelength and FWHM increases with increase of AS refractive index. Here, the obtained range is 74.17° to 79.27° and 6.64° to 7.41° for resonance angle and FWHM, respectively.

Figure 5, *a* and Fig. 5, *b* are showing the calculated sensitivity and FOM for SMTs and SMTb waveguide sensor at different AS refractive index respectively. It is noted that sensitivity varies from 20°/RIU to 30°/RIU for SMTs waveguide sensor while 35°/RIU to 50°/RIU for SMTb waveguide sensor. From the observation of numerical calculation, it is clear that SMTb waveguide sensor provides the high sensitivity in comparison of SMTs waveguide sensor. The maximum sensitivity is achieved 50°/RIU at 1.55 AS RI. Similar calculations have been done for finding the FOM at different RI of AS. It is clear that FOM varies from 6.15/RIU to 10.87RIU and 5.26/RIU to 6.74/RIU for SMTs and SMTb waveguide sensor, respectively. Here the SMTs sensor configuration provides the high FOM in comparison

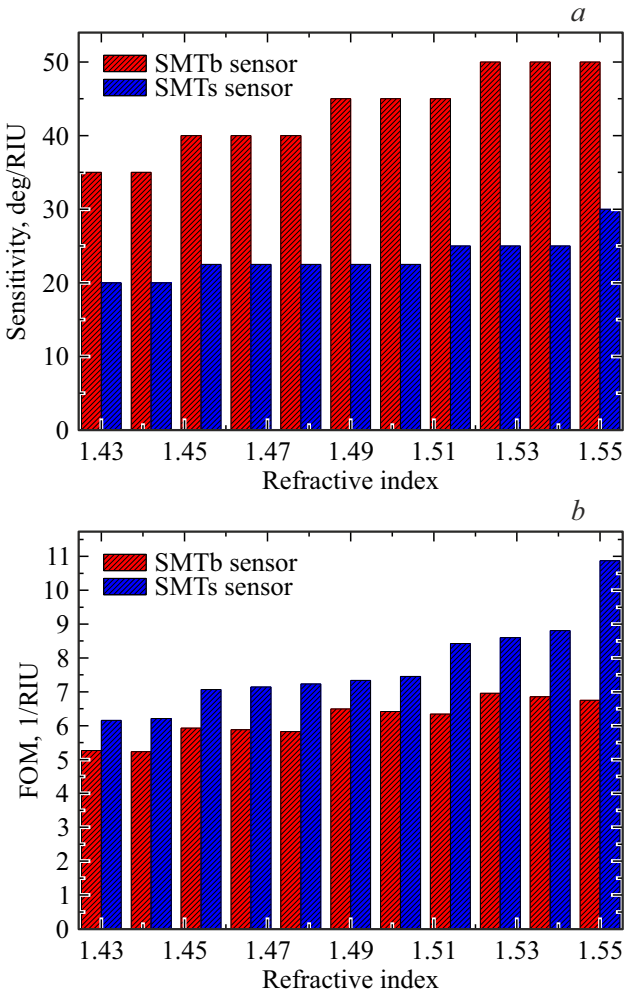

Figure 5. Numerical calculations of SMTs and SMTb waveguide sensor for (a) sensitivity and (b) FOM.

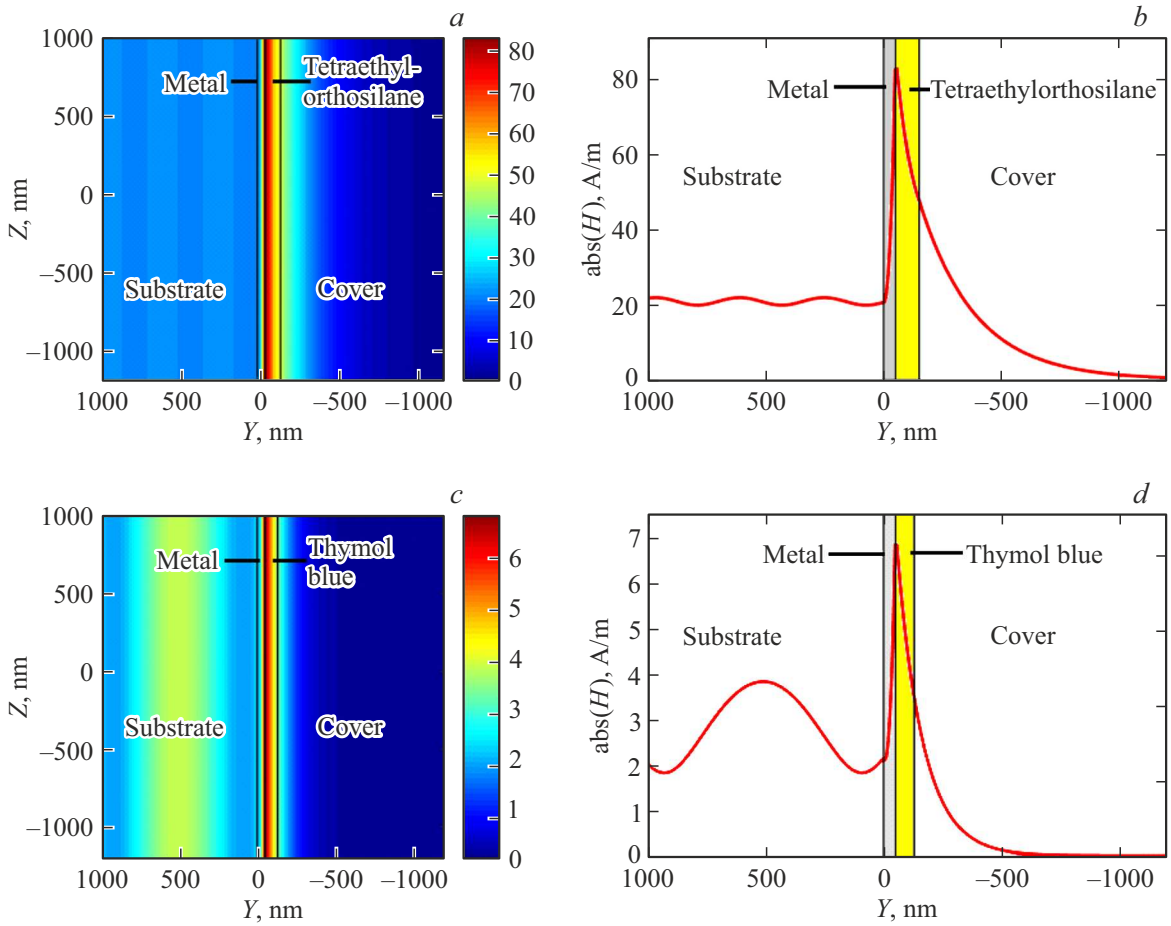

Figure 6. Calculated TM field pattern for SMTs waveguide sensor. (a) Contour map, (b) absolute field distribution and for SMTb waveguide sensor, (c) contour map, (d) absolute field distribution.

Table 2. The performance parameter for SMTs and SMTb waveguide sensor at considered three lower order modes

	SMTs sensor configuration				SMTb sensor configuration			
AS RI/ Mode	1.55		1.43		1.55		1.43	
	S, grad/RIU	*DA*, 1/grad	*S*, grad/RIU	*DA*, 1/grad	*S*,grad/RIU	*DA*, 1/grad	*S*, grad/RIU	*DA*, 1/grad
SPR	28.00	0.36	20.02	0.30	50.00	0.13	34.10	0.15
TM_1	0.50	0.29	00.22	0.29	4.80	0.14	Negligible	0.13
TM_2	0.80	0.29	Negligible	0.29	Negligible	0.13	Negligible	0.13

of SMTb sensor configuration. The maximum FOM is achieved 10.87/RIU at 1.55 AS refractive index. Further, it is also noted that sensitivity and FOM are increased as the increases of refractive index of AS. It is also instructive to calculate the field distributions of both waveguide sensor configurations. It is considered that incident wave exists in yz plane and travelling from $+y$ to $-y$. It is supposed that $+z$ axis holds substrate while metal, Ts/Tb film in the $-z$ direction. The field distribution is shown in Fig. 6 for SMTs and SMTb waveguides at calculated resonance angle 64.54° and 79.27°, respectively. Figure 6, a and Fig. 6, b show that the contour and absolute magnetic field in SMTs waveguide sensor for 1.55 AS refractive index. It is observed that intensities of radiation decay exponentially in cover region where AS is detected. The maximum absolute value of magnetic field at the interface (metal and film) and penetration depth of evanescent field in cover region is achieved 82 A/m and 1200 nm respectively. Similarly, the contour and absolute magnetic field for SMTb waveguide sensor is shown in Fig. 6, c and 6, d, respectively. Here, the obtainedmaximum absolute value of magnetic field is 7 A/m and penetration depth in cover region is attained 560 nm which is less than 1/2 times of SMTs waveguide sensor. The magnetic field strength in SMTs waveguide sensor is high more than 10 times in comparison of SMTb waveguide sensor. Therefore, it is concluded that SMTs

waveguide sensor provide better results in comparison of SMTb waveguide sensor configuration.

4. Conclusion

The performance of proposed surface plasmon resonance sensors having sol-gel film of Tetraethylorthosilane and Thymol blue for the detection of ammonium sulfates is estimated and compared. The dispersion characteristics are calculated for both waveguide sensor configurationsthat provide the cut-off thickness of sol-gel film for different mode of the waveguide. The cut-off sol-gel film thickness of SMTs and SMTb configuration for SPR mode is 100nm and 80nm respectively. The performance parameter of SPR sensor is calculated and compared. The obtained highest sensitivity is 50°/RIU for SMTb waveguide sensor and highest FOM is 10.87/RIU for SMTs waveguide. It is also noted that the magnetic field strength in SMTs waveguide sensor is high (more than 10 times) and penetration depth is high (more than 2 times) in comparison to SMTb waveguide sensor. Therefore, for detection of ammonium sulfate chemical aerosol the SMTs waveguide sensor configuration is recommended. It is also concluded that the ammonium sulfateaerosolsareoptimised using surface plasmon resonance sensor which will be highly encouraging in the field of aerosol sensing.

Acknowledgment

This work is supported by the project no. TAR/2019/000066, Science and Engineering Research Board (SERB), DSTNew Delhi India. The authors are grateful to Prof. R.D.S. Yadava, Physics Department, BHU, for their continuous encouragement. Dr Sushil Kumar is also thankful to Prof.MahendraNath Pandey their support in a well-mannered way.

Conflict of interest

The authors declare that they have no conflict of interest.

References

[1] S. Tiwari, A.K. Singh. Aerosol Air Qual. Res., **13**, 627–638 (2013).
[2] S. Tiwari et al. Envir. Sci. & Poll. Res., **25**, 24726–24745 (2018).
[3] M. Kuhnet et al. Geophysical Research Letters, **25**, 2679–2682 (1998).
[4] V.R. Oliver et al. Atmospheric Environment, **40**, 192–205 (2006).
[5] E. Carynelisa et al. J. Atmospheric Sciences, **68**, 1845–1852 (2011).
[6] F.G. Nicholas et al. Atmospheric Environment, **17**, 715–721 (1983).
[7] J.C. Holly, T.M. Scot. J. Geophysical Research, **106**, 1215–1226 (2001).
[8] K.J. Baustian, M.E. Wise, M.A. Tolbert. Atmos. Chem. Phys., **10**, 2307–2317 (2010).
[9] J. Surrat et al. Environ. Sci. Technol., **41**, 5363–5369 (2007).
[10] M. Jaoui et al. Anal. Chem., **76**, 4765–4778 (2004).
[11] A. Szmigielski et al. J. Mass Spectrom., **42**, 101–116 (2007).
[12] M. Kalberer et al. Science, **303**, 1659–1662 (2004).
[13] P. Laj et al. Atmos. Environ., **43**, 5351–5414 (2009).
[14] A. Kulkarnia et al. Sensors and Actuators B, **150**, 154–159 (2010).
[15] L.B. William. J. Optics A: Pure and Applied Optics, **8**, 87–93 (2006).
[16] A.A. Rifat et al. Sensor and Actuators B: Chemical, **243**, 311–325 (2017).
[17] S. Kumar, G. Sharma, V. Singh. Prog. in Electromagnetics Res., **37**, 167–176 (2013).
[18] S. Kumar et al. Silicon, **8**, 533–539 (2016).
[19] P. Yeh. Optical Wave in Layered Media (John Wiley & Sons, Inc. Publication, 2005).
[20] A.K. Sharma et al. J. Applied Physics, **107**, 034701 (2010).
[21] A.B. Petrin. Opt. Spectrosc., **125**, 390–397 (2018).
[22] S.K. Srivastava et al. Opt. Commun., **369**, 131–137 (2016).
[23] S. Kumar et al. Applied Physics A, **124**, 695 (2018).
[24] P. Chylek et al. J. Geophysical Research, **100**, 16325–16332 (1995).
[25] L. Jenny, M.K. Hand Sonia. Aerosol Science and Technology, **36**, 1012–1026 (2002).
[26] A.A. Riziq et al. Atmos. Chem. Phys., **7**, 1523–1536 (2007).
[27] J.G. Radney, C.D. Zangmeister. J. Quant. Spectrosc. Radiat. Transf., **220**, 52–66 (2018).